ELSEVIER

Chemical Engineering Journal 79 (2000) 123–131

Chemical Engineering Journal

www.elsevier.com/locate/cej

Identification of impact attrition mechanisms in solution by morphological analysis

Benoît Marrot[a], Marie-Noëlle Pons[b], Béatrice Biscans[a,*]

[a] *Laboratoire de Génie Chimique UMR 5503, CNRS/UPS/INPT/ENSIGC, 18 Chemin de la Loge, 31078 Toulouse Cedex 4, France*
[b] *Laboratoire des Sciences du Génie Chimique, CNRS-ENSIC-INPL, 1 rue Grandville, BP 451, 54001 Nancy Cedex, France*

Received 23 April 1999; received in revised form 22 March 2000; accepted 29 March 2000

Abstract

Image analysis was used to characterise quantitatively the shapes of single crystals impacted against a target. The conditions of impacts are created to simulate the impacts undergone by the crystals in an industrial crystalliser. The change of particle morphology due to attrition enables to understand the abrasion and breakage mechanisms of the crystals after one or several collisions. The projected area, the elongation, the robustness, the concavity characterise the evolution of the crystal shape as a function of the number of impacts. The crystal becomes rounded and its shape irregular. The quantification of the length and of the propagation of the created cracks is done. Cracks are initiated by the impacts and propagate to join one another, creating a fragment finally removed from the particle.

Keywords: Image analysis; Crystallisation; Attrition; Cracks; Morphology

1. Introduction

Attrition in industrial crystallisers is a process by which crystals abrade or break under the action of collisions between crystals, between the crystals and a part of the crystalliser, or under shear stress. Actually, it is a mechanical phenomenon that does not need any supersaturation of the solution to occur. The size, size distribution, surface and shape of the crystals can be modified by attrition, which can affect their end-use properties [1]. In a previous work, a specific experiment was developed to simulate impact attrition in crystallisers [2].

The aim of this study is to understand, by examining the morphology of particles, the mechanisms that induce crystal attrition. Morphology can be investigated by image analysis [3]. Automated image analysis permits to describe quantitatively shapes by a set of descriptors in a reproducible manner on a large number of particles. The crystal shape is analysed before and after the impact on a target. The length of the cracks developed on the surface of the crystal and their orientation in comparison with the face sides are quantified to understand the mechanisms of abrasion of the particle.

* Corresponding author. Tel.: +33-5-62-25-23-39; fax: +33-5-62-25-23-45.
E-mail address: beatrice.biscans@ensigct.fr (B. Biscans)

2. Materials and methods

2.1. Impaction device

The impaction device schematically represented in Fig. 1, was built in order to test the attrition propensity of single crystals. The velocities of impact developed in this experiment are those typically found in crystallisers for crystal/impeller impacts (between 2 and 10 m s^{-1}). In a crystalliser, all the dimensions of the impeller are larger than the crystal, and therefore, the contact can be assumed to be equivalent to the impact of a crystal on a flat target. Details on this experiment are given in the previous work [2,4]. The principle is to accelerate a single particle in a jet of saturated solution circulating in a vertical tube. The jet of solution carrying the particle penetrates into a vessel full of saturated solution in which a steel or a glass target has been immersed. The particle is impacted on the target and collected in a cylindrical chamber. The same particle can be impacted several times.

2.2. Generation of crystals

Single crystals of sodium chloride, chosen as a model, were grown by slow evaporation. The laboratory made crystals exhibit very few defects compared to industrial ones

1385-8947/00/$ – see front matter
PII: S1385-8947(00)00176-5

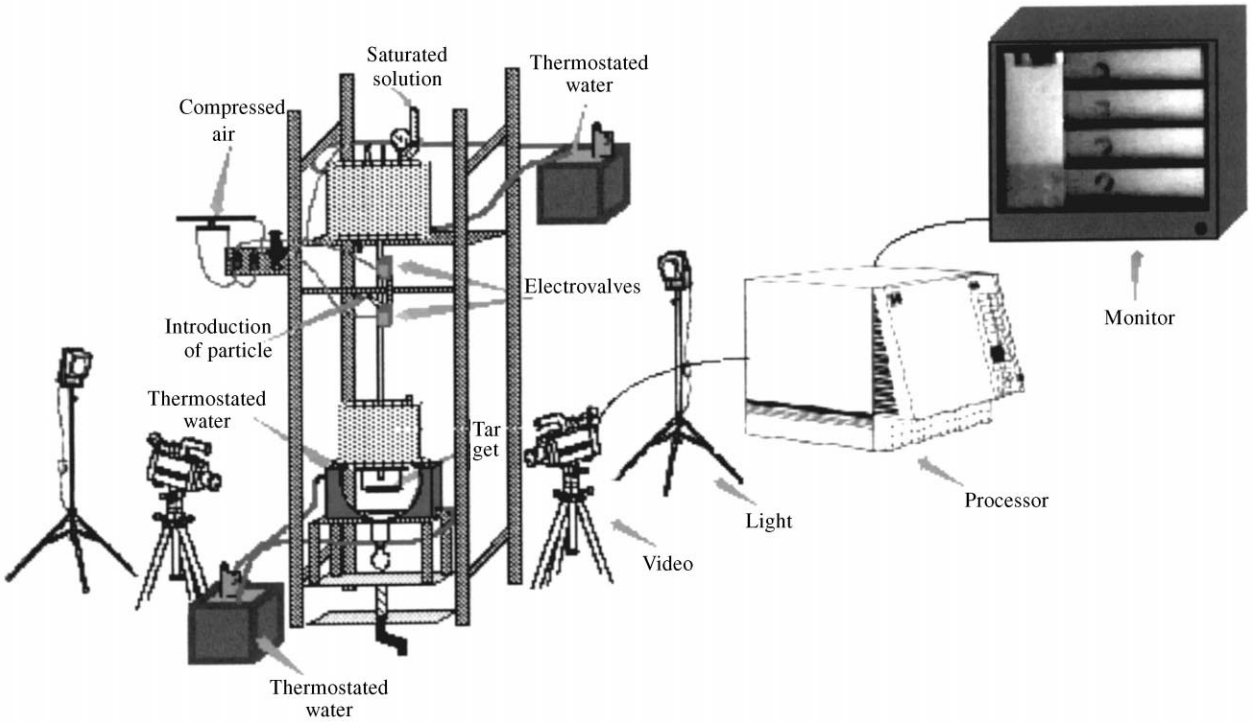

Fig. 1. Schematical representation of the impaction device.

which are already damaged. So, those more 'perfect' crystals are preferred in order to identify the defects actually due to impacts.

2.3. Visualisation of crystals

NaCl crystals have been visualised by three different methods as reported in Fig. 2:

- by light reflection (episcopy)
- by light transmission (diascopy)
- by scanning electron microscope (SEM).

The optical microscopy, working by episcopy or diascopy, is mainly useful to quantify the particles size and to follow the opacity evolution according to repeated impacts. In that case, the microscope is a Dialux, Leitz-Leica, with different lenses (2.5×, 10×). The images are captured via a video camera mounted on the microscope and connected to a SUN workstation via a SFG2200 grabbing board. The SEM (Jeol^{TM} 330A) working under an acceleration voltage of 5 kV and connected to a PC-compatible via an ImageSlave^{TM} board (Meeco, Melbourne, Australia) for direct capture of digital images, enables to reveal the cracks of gold-plated crystals and to determine their orientation according to the faces. It also enables to evaluate the loss of surface by means of the observed fragments. Images are later sent via the computer network to the workstation. 8-Bit grey-level images of 768×586 (light microscope) and 592×391 (SEM) square pixels are captured. A professional image analysis package Visilog^{TM} 4.1.4 (Noésis, Les Ulis, France) and lab-developed software are used.

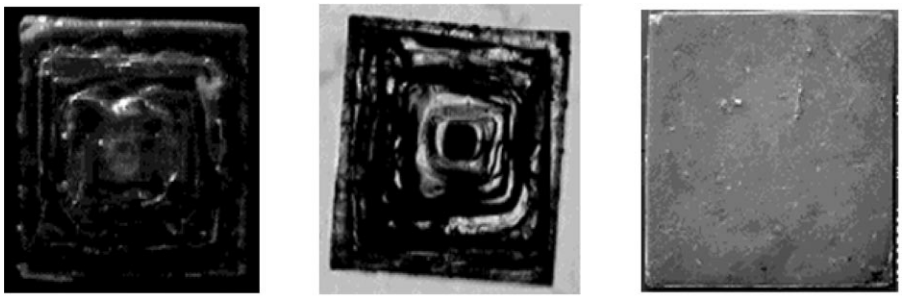

Fig. 2. Methods of visualisation of the particles.

Table 1
Shape descriptors

Macroscopic descriptors	Morphological descriptors
Elongation: $E = F_{max}/F_{min}$	Robustness: $\Omega_1 = 2\omega_1/\sqrt{S}$
Circularity: $C = P^2/4\pi S$	Largest concavity index: $\Omega_2 = 2\omega_2/\sqrt{S}$
Aspect ratio: $A = F_{max}/D_{eq}$	Concavity index: $CI = S/S_H$

2.4. Characterisation of the crystal shape

The characterisation of the crystal shape is based on two types of descriptors, which quantify, at different levels of details, the shape of the projected silhouette of the particle on the image plane (Table 1). They are invariant with respect to the size of the particle and to its position in the image. The equivalent diameter of the particle, D_{eq}, is calculated from its silhouette area, S

$$D_{eq} = 2\sqrt{\frac{S}{\pi}} \quad (1)$$

F_{max} and F_{min} are the maximal and minimal Feret diameters of the particle, respectively [5]. In the case of a square, F_{max} corresponds to the diagonal of the square and F_{min} to its side which gives E equal to 1.41 for a square and 1 for a disk. The aspect ratio of a square is equal to 1.25. P is the perimeter of the silhouette; the circularity of a square is 1.27. The particle silhouette is compared to its convex bounding polygon, of projected area S_H; ω_1 and ω_2 are the number of erosions necessary to eliminate completely the particle silhouette and its complement with respect to the reference shape, respectively [6]. The shape of reference for the robustness is the square, owing to the square mesh of the digital image. Ω_1 is equal to 1 for a square and to 0.8 for a disk. Ω_2 is equal to 0 for convex silhouettes but can take values larger than 1 for very concave shapes.

The silhouette construction depends on the type of image. The light microscopy images are first enhanced by a morphological gradient in order to sharpen the contour of the crystal. After thresholding of the contour, defects may remain. Some images obtained by light reflection, especially those showing a small number of impacts, let appear a contour which is not closed. A manual editing of the image by the operator is necessary.

For the crystals observed by light transmission, the contour is quite contrasted, except for some crystals, i.e. those that are very transparent. Again, a manual check of the contour by the operator is necessary. Once the contour is closed, the silhouette is automatically built by filling of the contour.

The images from the SEM are used for the characterisation of the cracks and of the fragments detached from the crystals surface (Fig. 3). The operator draws with a cursor, the contours of the crystals and the fragments; then these contours are filled. The previously described shape characterisation is here applied to the crystal and to the fragments.

The cracks are also drawn manually with the cursor and the corresponding lines are transformed into vectors, the characteristics of which will enable to determine the position of the cracks with respect to the crystal faces.

3. Results and discussion

3.1. Morphological evolution of a single particle undergoing several impacts

The same particle has undergone several successive impacts: 0, 1, 5, 10, 15, 20 and 30. In this experiment, the velocity of impact was $7.5\,m\,s^{-1}$ and the target was made out of glass. The hardness of this target has been measured by the Vickers method [4] to be equal to 5.0×10^9 Pa. This target is 30 times harder than the NaCl particles which have a hardness of 171×10^6 Pa. Methods for measuring crystal hardness are developed in the literature [7,8].

The images of each face of the crystal, from the first to the 30th and last impact, enable to detect the phenomena following each impact. The morphological evolution of the crystal according to the number of impacts is presented on Fig. 4.

3.1.1. The surface

It can be noticed on Fig. 5, reporting the surface of the particle face (in pixels) as a function of the number of

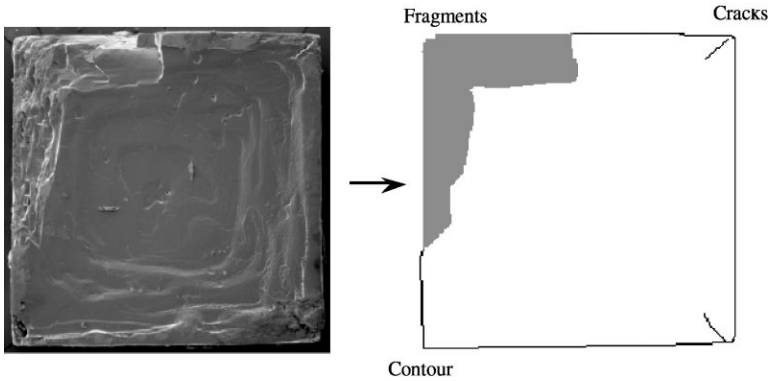

Fig. 3. Procedure of shape characterisation for SEM images.

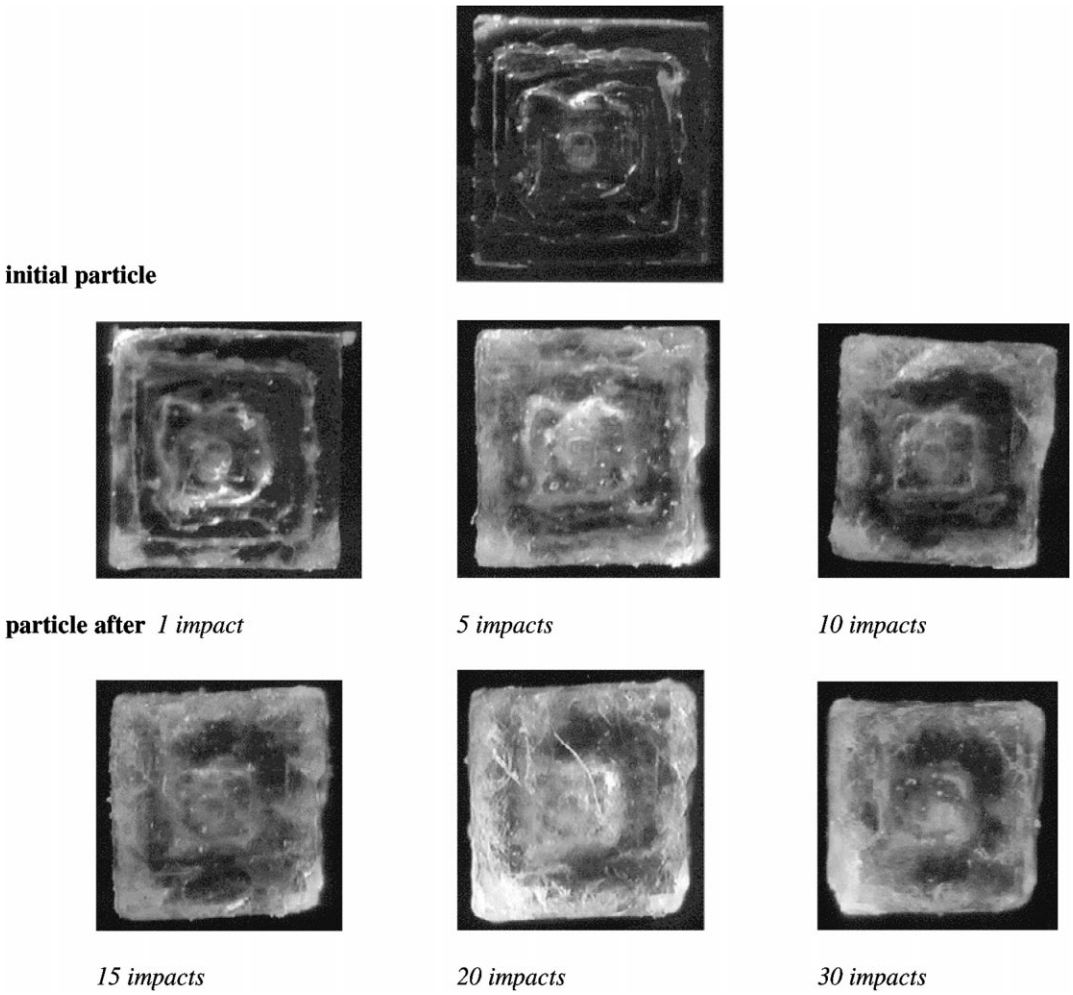

Fig. 4. Morphological evolution of the crystal according to the number of impacts.

impacts, that this surface decreases by 12.5% after 30 impacts. The surface loss is approximately the same for each face. Under this assumption the volume is equal to [$V = (\sqrt{S})^3$], and the volume loss after 30 impacts would be of 18.20%. This number can be compared to the difference of mass of the single crystal before and after the 30 impacts and which is on the average of 24.63%.

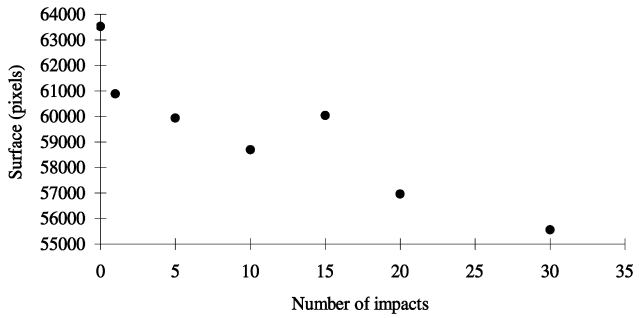

Fig. 5. Evolution of the crystal surface according to the number of impacts.

3.1.2. The elongation and robustness

The elongation (Table 1) decreases on Fig. 6, from 1.42 (close to the theoretical value of a square) to 1.32. It shows that the angles become more rounded. The more the particle is impacted, the more it becomes round and irregular. This trend is confirmed by the evolution of the crystal robustness

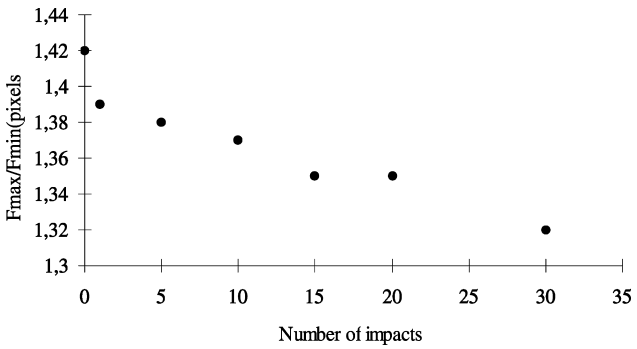

Fig. 6. Evolution of the crystal elongation according to the number of impacts.

Table 2
Number of crystals treated for each series of impacts

No. of impacts	No. of crystals
0	11
1	9
2	7
3	6
5	7
10	7
20	5

Ω_1. Under the effect of repeated impacts, the robustness of the crystal decreases from 0.95 for the initial crystal to 0.92 after 30 impacts.

3.1.3. The concavity index

The number of impacts does not have any influence on the concavity index, the value of which remains around 0.99 during the 30 impacts. This can be explained by the fact that abrasion of the crystal is dominant over fragmentation during the 30 considered impacts. This abrasion does not create any concavity on the crystal shape.

3.2. Morphological evolution of different particles undergoing several impacts

In this set of experiments, several individual particles are impacted. The mass and size of each particle differ slightly, in the range 3–10 mg. The impact velocity for all the trials is $7.5\,m\,s^{-1}$ on a target which is made of steel and has an hardness equal to 2×10^9 Pa, i.e. 12 times harder than the particles [4]. The conditions of impacts are reported on Table 2. As previously, the different morphological and macroscopic descriptors are used to quantify the attrition.

3.2.1. The circularity

The average circularity varies according to the number of impacts as described in Fig. 7. It decreases from an initial value close to the theoretical value obtained for a perfect square (1.27), toward 1.00 which is the value obtained for a disc. The increase noticed for the small number of impacts

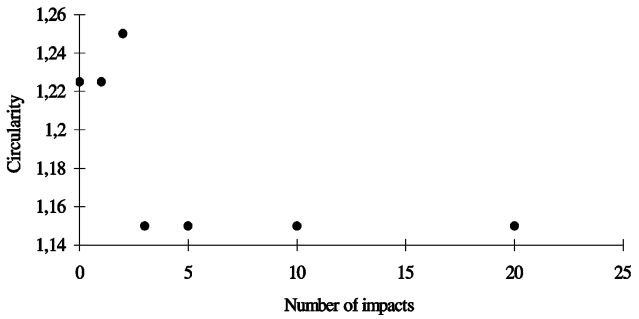

Fig. 7. Evolution of the crystal circularity (averaged values) according to the number of impacts.

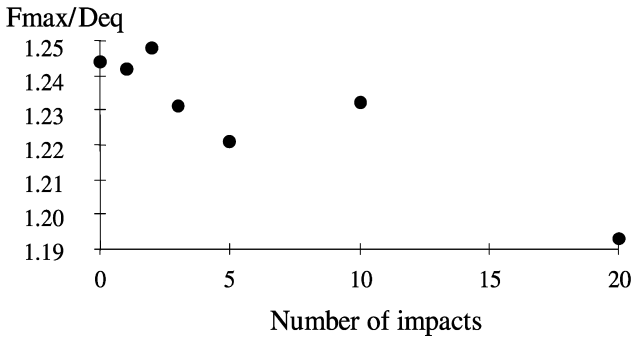

Fig. 8. Evolution of the aspect ratio according to the number of impacts.

is the result of the loss of fragments by some particles, the circularity being sensitive not only to the elongation of the particle but also to its roughness.

3.2.2. The elongation and the aspect ratio

The average elongation increases at the beginning of series of impacts, because of the fragmentation of an angle of the cubic crystal. This is in agreement with what was observed with the circularity. Then, the elongation decreases when the other angles of the particle are suppressed and the shape becomes rounded. From an initial value of 1.41, it becomes equal to 1.36 and shows that the first sites of fragmentation are the corners of the particles.

The aspect ratio, F_{max}/D_{eq}, is another global index quantifying the shape of the particles and is given in Fig. 8. During the first impacts, a small increase of the ratio, followed by a decrease occurs, except for the 10th impact. This concerns a crystal in the mass range 5–6 mg and for which F_{max}/D_{eq} is equal to 1.3. This difference of value in comparison with the other ones comes from the fact that an angle of the crystal is entirely broken and this leads to a 'rectangularisation' of the shape. Globally, in the absence of breakage, this index confirms the change of crystals shape: initially similar to a square, the particles become progressively rounded.

3.2.3. The transparency

The average grey level value of the crystal is related to the transparency of the crystal: when observed by light transmission opaque crystals appear black (low grey levels) and transparent ones are clear (high grey levels).

Fig. 9 gives the values of grey level as a function of the number of impacts. A decrease of the grey level is observed when the number of collisions increases, as the crystal becomes less and less transparent. The grey level of the crystals decreases of about 32% after 10 impacts. The change in transparency could result from the ions displacement from their original position, which creates inside the crystal some dislocations and/or deficiency.

The average grey level seems to become stabilised after about 10 impacts. Two explanations could justify this phenomenon:

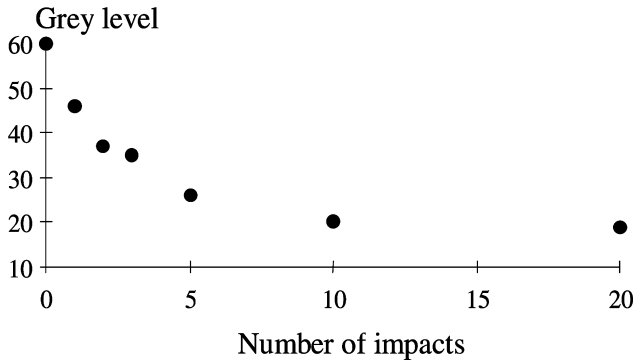

Fig. 9. Evolution of the crystal grey level according to the number of impacts (average values on several particles).

- either the camera is no longer able to distinguish the grey level variations. It depends on the range of levels and on the light setting;
- or, this means that the position of ions are changed during the first impacts and that after these impacts, the ions have such a configuration that they cannot move anymore. This could explain that the next impact leads to fragmentation.

It could be useful at that stage to consider the energy transmitted to the crystal during the impact. First, this energy can be used to displace the ions by creating dislocations. Under the imposed constraints, many dislocations can develop near the surface of the crystal and create a crack. Then, when the ions are not able to move any more because they have reached a stable position, the subsequent impacts can break some bonds, provoking the birth of cracks and fragments. Barenblatt [9] admits that in front of the visible crack, an area exists, in which the atoms or molecules can be moved away from each other.

3.3. Analysis of fragments

The analysis of the fragment number, projected area and shape was performed on the SEM images. This concerns only the thin chips removed from the surface, which leave visible marks on the crystal. Until the fifth impact an increasing number of fragments appears anywhere on the crystal surface (Fig. 10). Then, the number decreases but the fragments reduced area (calculated as a fraction of the crystal face area), which remains quasi-constant for the first impacts increases strongly. This may be due to the junction of different fragments but also to the fact that the first impacts may just induce some fatigue of the particle with a limited removal of small fragments; then, the defects in the crystal are such that large fragments are removed. Fig. 11 shows the displacement of the zone of the plane Ω_1 versus Ω_2 representative of the fragments, in function of the number of impacts. The fragments obtained after one impact are rather convex with a high robustness. Then they become more elongated and concave. After 20 impacts, large and very concave fragments are removed from the crystals.

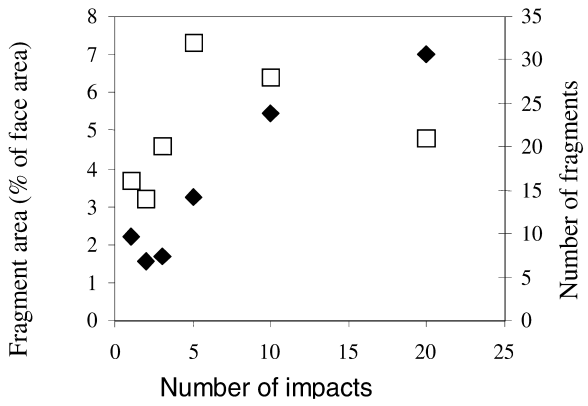

Fig. 10. Effect of the number of impacts on the number (❑) and projected area (◆) of the fragments.

3.4. Cracks quantification

Taking into account the particle characteristics, the constraints distributed inside the particle determine the future cracks network. The density and the orientation of the cracks influence both the dimension and the shape of the fragments. The image analysis allows the characterisation of the cracks in order to understand their evolution.

Because of the fluctuating turbulence in the liquid phase, the particles are almost randomly oriented in the vicinity of the target. Contact with corners are therefore most likely and result in higher local stresses due to the smaller area of contact. On Fig. 3, the cracks on the crystal are seen to emanate from the region adjacent to the plastically deformed zone. For NaCl, these cracks usually start in ⟨1 1 1⟩ direction.

Some examples, taken among the obtained results, are presented in Fig. 12 in which all the crystals are different and the co-ordinates are given in pixels. The figure shows that, as for the crystals observed by light microscopy, the shape of the crystals become irregular as the number of impacts increases. The number of created cracks increases up to the fifth impact and then decreases. The fifth impact is the one that presents the largest number of cracks, but it is also at

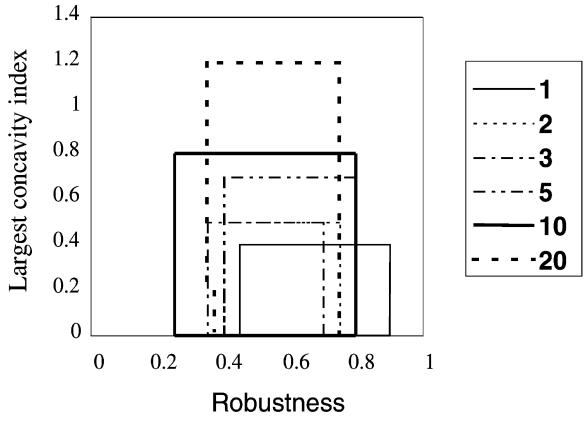

Fig. 11. Effect of the number of impacts on the shape of the fragments.

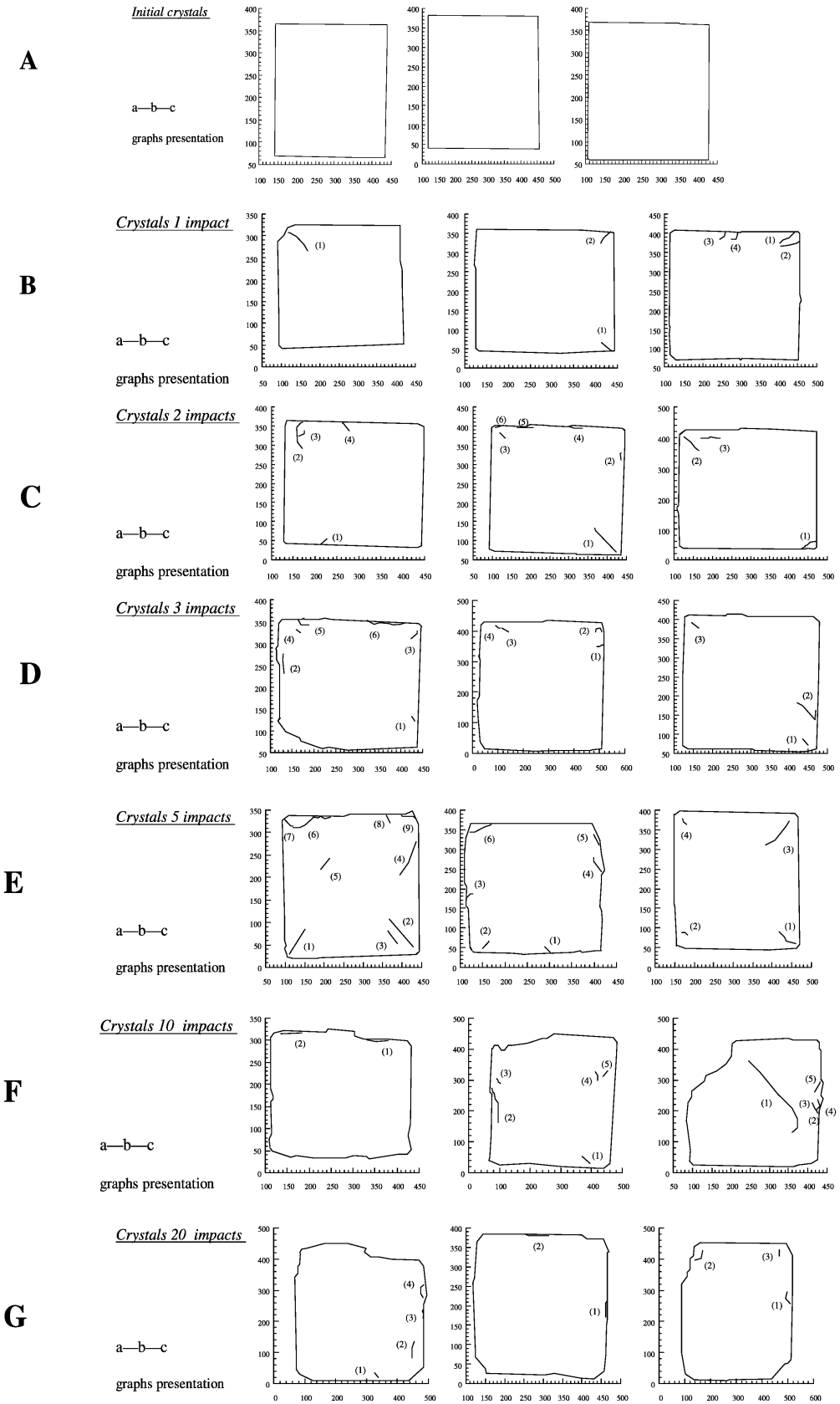

Fig. 12. Shape of the crystals: (A) initial crystals; (B) cracks in surface after one impact; (C) cracks in surface after two impacts; (D) cracks in surface after three impacts; (E) cracks in surface after five impacts; (F) cracks in surface after 10 impacts and (G) cracks in surface after 20 impacts.

the fifth impact that the cracks are the most widespread on the face. The average fragment projected area is 0.13% of the crystal face area at the first impact and 0.10% at the fifth impact. It then increases to reach 0.33% after 20 impacts.

After two impacts (Fig. 12C), few cracks are observed. For particles impacted 3, 5 and 10 times, some cracks have joined to create a single one (Fig. 12D–F). Moreover, after the 10th impact, when the particle is broken, the crack does not appear around the site of impact (Fig. 12F and G).

As previously observed, the propagation of the cracks and their junction weaken the particle, and the next collision generates a fragment. Other important cracks are not immediately created on the broken site.

The cracks are individually analysed and characterised by the following three parameters:

- the crack angle according to the crystal side,
- the variation of the crack angle during its propagation and
- the crack length.

For all the crystals examined, most of the cracks formed an angle between 40 and 50° with the closest face side, whatever the number of impacts. Then, the crack deviates. The deviation angle does not seem to be linked either to the number of impacts, or to the crack length. This deviation often follows the surface irregularities. The crack does not propagate necessarily linearly. Irwin [10] showed that the way a crack extends only depends on the stresses generated and on the distortion created around the crack front.

The angle of deviation of the cracks has been quantified. Then, it becomes possible to classify the number of cracks with an angular interval of 10°, for example, 90–80°, 80–70°, . . . , etc. In most cases, the crack deviation belongs to the range 20–50°; and very few cracks have a deviation larger than 60°.

The crack length does not depend either on the angle at its generation, or on the angle of deviation during its propagation. On the contrary, the crack length seems to be influenced by the number of impacts as shown on Fig. 13.

The crack average length increases until the fifth impact and then decreases slightly. This confirms that the first five impacts create cracks disseminated all over the crystal and that the impacts occurring later enable their propagation until they create fragments and disappear; that is the reason why the average length decreases. Nevertheless, in spite of the fragmentation, the cracks generated on the 10th and 20th impacts remain on average longer than those born during the first collisions.

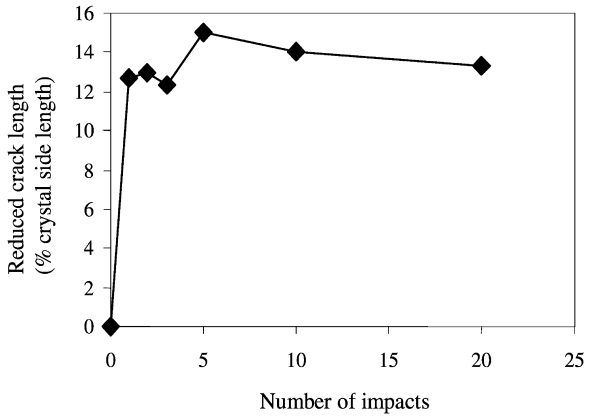

Fig. 13. Average length of the cracks as a function of the number of impacts.

4. Conclusions

This study on the mechanisms of attrition of crystals due to impact has used two methods based on image analysis. Image analysis is an interesting way to quantify these effects as it enables, by a direct observation of the particles, to calculate some descriptive parameters that can be linked to the operating parameters and that bring to the fore an attrition mechanism. Nevertheless, a preliminary phase of development and of adaptation to the objectives of the study has been necessary. It concerns the image treatment and the choice of the measured parameters. In the first part, the morphological changes undergone by the crystals as a function of the number of impacts against the target have been quantified on light micrographs. The analysis of the crystal surface and the quantification of its change in function also of the number of impacts has been performed on scanning electron micrographs, by means of characterisation of the observed cracks and fragments. These quantitative aspects enable to have a better insight into the relationships between the morphological and operational parameters.

On particles submitted to repeated impacts, either on a glass or a steel target, the parameters of surface, elongation, robustness, concavity show the evolution of the crystal shape according to the abrasion it is subject to. It becomes rounded and its shape becomes irregular. The grey level is a quantification of the increase of the particle opacity during the impacts. This parameter can be a macroscopic quantification of the changes occurring at the microscopic level. Actually, the crystal impact can provoke changes at the molecular level, the intensity of which could depend on the number of impacts.

Moreover, the quantification of the created cracks by SEM shows that during the first impacts the cracks are generated, then develop on the crystal surface and then disappear. At first, these cracks make the particle fragile and they disappear during a next collision creating a fragment, without making other cracks appear around the impacted site.

In the future work, powerful microscope (atomic force microscope) will be used to allow characterisation of the internal structure of the crystals, before and after the impacts.

5. Nomenclature

C	circularity
CI	surface concavity index

D_{eq}	equivalent diameter (m)
F_{max}	maximal Feret diameter (m)
F_{min}	minimal Feret diameter (m)
P	perimeter (m)
S	surface (m^2 or pixels)
S_H	surface convex hull (m^2 or pixels)
V	volume (m^3)

Greek symbols

Ω_1	particle robustness
Ω_2	largest concavity
ω_1	no. of erosions necessary to eliminate completely the particle silhouette
ω_2	no. of erosions necessary to eliminate the residual set

References

[1] A. Chianese, R.G. Saugl, A.B. Mersmann, On the size distribution of fragments generated by crystal collisions, Chem. Eng. Commun. 146 (1996) 1–12.

[2] B. Marrot, B. Biscans, Impact attrition rates in suspension: experimental and theoretical approach, World Congress on Particle Technology, Vol. 3, ISBN 0-85295-401-8, 1998, pp. 8–16.

[3] H. Vivier, M.N. Pons, B. Bernard-Michel, T. Rolland, L. Voignier, M. Vucak, Quantification of particle morphology in powder process technology, Microsc. Microanal. Microstruct. 7 (1996) 467–475.

[4] B. Marrot, B. Biscans, Impact attrition of sodium chloride crystal in saturated solution: single particle impact experiment. Comparison with indentation experiment, in: Proceedings of the 13th Symposium on Industrial Crystallisation, Vol. 2, 1996, pp. 491–496.

[5] M. Vucak, J. Peric, M.N. Pons, H. Vivier, Effect of precipitation conditions on the morphology of calcium carbonate: quantification of crystal shapes using image analysis, Powder Technol. 97 (1998) 1–5.

[6] M.N. Pons, H. Vivier, J. Dodds, Particle shape characterisation using morphological descriptors, Part. Syst. Charact. 14 (1997) 272–277.

[7] J. Engelhardt, S. Haussühl, Fortschr. Miner. 42 (1965) 1–5.

[8] J. Ulrich, M. Kruse, Ultra-micro-hardness of organic and inorganic crystals, J. Phys. D. Appl. Phys. 26 (1993) B168–B171.

[9] G.I. Barenblatt, The mathematical theory of equilibrium cracks in brittle fracture, Adv. Appl. Mech. 7 (1962).

[10] G.R. Irwin, Fracture handbuck der physik, Ed. Flugge 6 (1956) 551–590.